Journal of Applied Mathematics and Physics, 2014, 2, 1123-1129
Published Online November 2014 in SciRes. http://www.scirp.org/journal/jamp
http://dx.doi.org/10.4236/jamp.2014.212131

Numerical Investigation of the Tri-Atomic Ions Formation during Laser Ionization Based on Resonance Saturation

M. A. Abdelati[1], M. A. Mahmoud[2], Y. E. E. Gamal[1]

[1]National Institute of Laser Enhanced Sciences, Cairo University, El Giza, Egypt
[2]Physics Department, Faculty of Science, Sohag University, Sohag, Egypt
Email: maa@niles.edu.eg

Received August 2014

Abstract

We present a theoretical investigation of plasma generation in sodium vapor induced by laser radiation tuned to the first resonance line (3S-3P) at λ = 589 ns. A set of rate equations that describe the rate of change of the ground and excited states population as well as the temporal variation of the electron energy distribution function (EEDF), beside the formed atomic ion Na^+, molecular ion Na_2^+ and tri-atomic ions Na_3^+ are solved numerically. The calculations are carried out at different laser energy and different sodium atomic vapor densities under the experimental conditions of Tapalian and Smith (1993) to test the existence of the formed tri-atomic ions. The numerical calculations of the electron energy distribution function (EEDF) show that a deviation from the Maxwellian distribution due to the super elastic collisions effect. In addition to the competition between associative ionization (3P-3P), associative ionization (3P-3D) and Molnar-Hornbeck ionization processes for producing Na_2^+, the calculations have also shown that the atomic ions Na^+ are formed through the Penning ionization and photoionization processes. These results are found to be consistent with the experimental observations.

Keywords

Plasma, Laser, Collisional Ionization, Association Ionization, Tri-Atomic Ions, Photoionization, Electron Energy Distribution Function

1. Introduction

Resonant laser excitation has played a vital role in coupling energy into vapor where efficient ionization by resonance saturation has been observed in Alkali-metal vapor. This phenomenon has attracted the attention of many authors due to its importance in different fields such as astrophysics, plasma physics and photochemistry [1]-[7]. Plasma generation induced by intense laser radiation under such conditions showed high efficiency when the laser wavelength corresponds to an absorption line of the ionized alkali-vapor. Such interaction involves many collisional ionization and excitation energy as well as radiative transfer processes [16] [17]. Accor-

How to cite this paper: Abdelati, M.A., Mahmoud, M.A. and Gamal, Y.E.E. (2014) Numerical Investigation of the Tri-Atomic Ions Formation during Laser Ionization Based on Resonance Saturation. *Journal of Applied Mathematics and Physics*, **2**, 1123-1129. http://dx.doi.org/10.4236/jamp.2014.212131

dingly in the present work a theoretical study is under taken to investigate the formation of triatomic ions by tuning a laser source to the transition 3p-4d at a wavelength 569 nm in laser excited sodium vapor at the first resonance transition $3s_{1/2}$-$3p_{1/2}$. The formation of this process is found to depend mainly on the associative ionization reaction given by [7]: $\mathrm{Na}(4\mathrm{d})+\mathrm{Na}_2 \to \mathrm{Na}_3^+ + \mathrm{e}^-$ in this reaction Na_2 is assumed to be present at 0.5% percent in the sodium atomic beam. This study based on a model which solves numerically a set of rate equations that describe the temporal variation of the following parameters: the electron energy distribution function, the electron density, the population of the states 3s, 3p and 4d. The temporal variation of Na^+, Na_2^+ and Na_3^+ are also involved. These calculations are carried out for various sodium atomic densities. The model includes electron generating processes as well as electron heating processes.

2. Rate Equations

The calculations are based on the system of rate equations similar to those presented in our previous papers [8] [9]. A set of coupled differential equations" which describe the instantaneous population densities of the considered energy states", electron density as a function of electron energy together with the normalization conditions are developed and solved iteratively. Accordingly the equations which represent the rate of change of instantaneous population density of 3S, 3P and N (n) states are given by:

$$\begin{aligned}\frac{\mathrm{d}N(3S)}{\mathrm{d}t} &= N(3P)(R_{21}+A_{21}) - N(3S)R_{12} + \int n_e(\varepsilon)N(3P)K_{21}(\varepsilon)\mathrm{d}\varepsilon \\ &\quad - \int n_e(\varepsilon)N(3S)K_{12}(\varepsilon) + N(3P)N(n)K_{\mathrm{PI}} \\ &\quad + \frac{1}{2}N^2(3P)K_{\mathrm{EP}} - N(n)N(3S)K_{\mathrm{HMI}} - N(3S)n_e(\varepsilon)K_{1c}(\varepsilon).\end{aligned} \tag{1}$$

$$\begin{aligned}\frac{\mathrm{d}N(3P)}{\mathrm{d}t} &= N(3S)R_{12} - N(3P)(R_{21}+A_{21}) - \int n_e(\varepsilon)N(3P)K_{21}(\varepsilon)\mathrm{d}\varepsilon + \int n_e(\varepsilon)N(3S)K_{12}(\varepsilon)\mathrm{d}\varepsilon \\ &\quad - \frac{1}{2}N^2(3P)K_{\mathrm{AI1}} - N(3P)N(3D)K_{\mathrm{AI2}} - N(3P)N(n)K_{\mathrm{PI}} - \frac{1}{2}N(3P)^2\sigma_{\mathrm{PL}}vF \\ &\quad - \frac{1}{2}N^2(3P)K_{\mathrm{EP}} - N(3P)\sigma_{2c}^{(2)}F^2 - N(3S)n_e(\varepsilon)K_{2c}(\varepsilon) - N(3P)R_{26}.\end{aligned} \tag{2}$$

$$\begin{aligned}\frac{\mathrm{d}N(n)}{\mathrm{d}t} &= \sum_{n\succ m} n_e(\varepsilon)N(n)K_{nm}(\varepsilon) - \sum_{m\succ n} n_e N(n)K_{mn}(\varepsilon) - \sum_{n\succ m} A_{nm}N(n) - \sum_{n} n_e(\varepsilon)N(n)K_{nc}(\varepsilon) \\ &\quad - \sum_{n} N(3P)N(n)K_{\mathrm{PI}} + \frac{1}{2}N^2(3P)K_{\mathrm{EP}} - \sum_{n} N(n)N(3S)K_{\mathrm{HMI}} - \sum_{n\supset 2} N(n)\sigma_{nc}^{(1)}F \\ &\quad + N_{\mathrm{Na}^+}n_e(\varepsilon)\sum_{n}\left[n_e(\varepsilon)K_{cn}(\varepsilon) + K_{RD}(\varepsilon)\right] + N(3P)R_{26} - N(4d)N(\mathrm{Na}_2)K_{4d+\mathrm{Na}_2}.\end{aligned} \tag{3}$$

While the rate of growth of the molecular ion, atomic ion and the tri-atomic ions is given by

$$\frac{\mathrm{d}N(\mathrm{Na}_2^+)}{\mathrm{d}t} = \frac{1}{2}N^2(3P)K_{\mathrm{AI}} + N(3P)N(3D)K_{\mathrm{AI2}} + N(n)N(3S)K_{\mathrm{HMI}} \tag{4}$$

$$\frac{\mathrm{d}N(\mathrm{Na}^+)}{\mathrm{d}t} = N(3P)N(n)K_{\mathrm{PI}} + \frac{1}{2}N(3P)^2\sigma_{\mathrm{PL}}vF + N(3P)\sigma_{2c}^{(2)}F^2 + \sum_{n\supset 2}N(n)\sigma_{nc}^{(1)}F \tag{5}$$

$$\frac{\mathrm{d}N(\mathrm{Na}_3^+)}{\mathrm{d}t} = N(4d)N(\mathrm{Na}_2)K_{4d+\mathrm{Na}_2} \tag{6}$$

where R_{21} (sec^{-1}) represents the stimulated emission rate coefficient for transition from level 2 to 1.

$$R_{21} \equiv B_{21}\int I(\nu)L_{21}(\nu)\mathrm{d}\nu/4\pi \cong (I/h\nu)\sigma_{21}(\upsilon),$$

$I(\nu)$ is the spectral irradiance of the radiation field at frequency ν appropriate to the $2 \to 1$ transition, B_{21} represents Milne coefficient, and L_{21} (ν) represents the corresponding line profile function for the transition. R_{26}

(sec^{-1}) represents the stimulated emission rate coefficient for transition from level 2 to 6. A_{21} is the resonance transition Einstein coefficient for spontaneous emission. $N(3S)$, $N(3P)$ and $N(n)$ represents the population density of levels 3S, 3P and nl respectively. ne (ε) represents the free electron density as a function of electron energy ε. K_{mn} ($cm^3.sec^{-1}$) represents the electron-collision rate coefficient for electron-atom collisional excitation or de excitation between the states *m* and *n* (the former was calculated by Measure's formula [10] and the latter employing detailed balance relations). K_{nc} ($cm^3.sec^{-1}$) represents the electron collisional ionization rate coefficient for level *n* calculated by Vriens and Smeets [11] and K_{cn} ($cm^6.sec^{-1}$) represents the three body recombination rate coefficient calculated from the detailed balance relations.]. K_{RD}($cm^3.sec^{-1}$) represents the radiative recombination rate coefficient to level *n* determined by Darwin and Felenbok [12]. K_{AI1}, K_{AI2}, K_{MHI}, K_{PI} and K_{EP} are the rate coefficients of associative ionization (3p-3p), associative ionization (3p-3d) [13], Hornbeck-Molnar ionization [14], Penning ionization [2] and energy pooling collisions [15] [16] respectively. $\sigma_{nc}^{(1)}$ is the single-photon ionization cross section for level *n* [17], $\sigma_{2c}^{(2)}$ is the two photon [18], resonance state ionization cross section and σ_{PL} is laser induced Penning ionization cross section [19] and *v* is average velocity of atoms Units, in cm/sec $v=\sqrt{\frac{kT}{m}}=2.688\times10^{3}\sqrt{K^{o}}$ T is the temperature of saturated vapor. F represents the photon flux density. In Equation (6) $K_{4d+\mathrm{Na}_2}$ represents the triatomic associative ionization rate coefficient [7]. The time evolution of the electron energy distribution function is given by Boltzmann equation including all the collisional processes in which the plasma electrons are involved

$$
\begin{aligned}
\frac{\mathrm{d}n_e(\varepsilon)}{\mathrm{d}t} &= \sum_{m\supset n} n_e(\varepsilon)N(m)K_{nm}(\varepsilon)-\sum_{m\subset n} n_e(\varepsilon)K_{mn}(\varepsilon)+\sum_{n} n_e(\varepsilon)N(n)K_{nc}(\varepsilon)+\sum_{n} N(3P)N(n)K_{\mathrm{PI}} \\
&\quad +N(3P)\sigma_{2c}^{(2)}F^2+\sum_{n\supset 2} N(n)\sigma_{nc}^{(1)}F+\frac{1}{2}N^2(3P)K_{\mathrm{AI1}}+N(3P)N(3D)K_{\mathrm{AI2}}+\frac{1}{2}N(3P)vF \\
&\quad +\sum_{n} N(n)N(3S)K_{\mathrm{HMI}}-N_{\mathrm{Na}^+}n_e(\varepsilon)\sum_{n}\left[n_e(\varepsilon)K_{cn}(\varepsilon)+K_{\mathrm{RD}}(\varepsilon)\right]+N(4d)N(\mathrm{Na}_2)K_{4d+\mathrm{Na}_2}.
\end{aligned}
\tag{7}
$$

The normalization conditions are

$$N_0=\sum_{n} N(n)+N(\mathrm{Na}^+) \tag{8}$$

$$\int_0^\infty n_e(\varepsilon)\varepsilon^{1/2}\mathrm{d}\varepsilon=1,\quad \int_0^\infty n_e(\varepsilon)\mathrm{d}\varepsilon=N_e \tag{9}$$

where N_e is the number density of electrons and N_0 is the density of Na vapor. Note that the factor 1/2 with K_{EP} and K_{AI} corrects for possible double counting of each colliding pair of identical particles [20].

The rate coefficients of collisional ionization processes and the cross sections of the photoionization processes in our model are adopted from our previous paper [9]. The rate constant of the Na_3^+ formations is taken from the measurements that carried out in [7].

3. Results and Discussions

The above shown set of Equations (1)-(9) are solved numerically using the Rung-Kutta fourth-order technique under the experimental conditions of Tapalian and Smith (1993) [7]. In their experiment, they examined a plasma formed by a resonant CW laser at different atomic densities of sodium. A computer program is under taken to obtain the following relations 1) The population of Na_3^+ and Na_2^+ as a function of the sodium atomic density at different exposed times. 2) The time evolution of the (4d) state in the presence and absence of the triatomic associative ionization process as a function of a sodium atomic density. 2) Electron energy distribution functions for different values of both sodium atomic density and exposure time in the presence and absence of triatomic associative ionization process.

3.1. Dependence of Na_3^+ and Na_2^+ on Sodium Vapor Density

There is a clear correlation between the growths of Tri-atomic ions with the Sodium atomic density, since the growth of Na^3 start slowly at the low atomic density up to 1.5×10^{12} cm^{-3} then it followed by a noticeable increase as shown in the **Figure 1(a)**. This behavior is observed over the whole range of the exposure time. It is

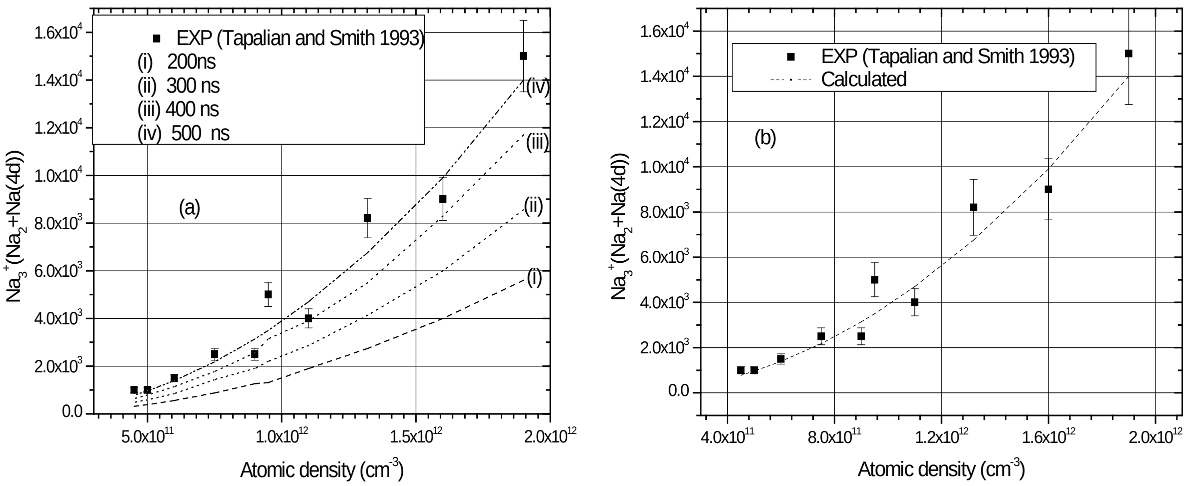

Figure 1. Na_3^+ ion yield versus atomic density.

also noticed here that the most closer calculated values of the Na^3 to the experimentally measured ones are those obtained at exposure time 500 ns. The agreement shown in this **Figure 1(b)** assures the validity of the model. The variation of the formed molecular ions density against the Sodium atomic density is shown in the **Figure 2**. For an easy comparison the experimentally measured ones of Tapalian and Smith [7] are also shown in this figure. It is noticed here that the molecular ions density increases with the increase of the atomic density this is observed for both calculated and measured values.

In addition molecular ions can also be formed through photo – ionization of Sodium molecules. The generation of these ions increases linearly with the atomic density as shown in **Figure 3**.

3.2. The Effect of Triatomic Formation on the Population Density of the 4d State

The formation of Tri atomic ions depends mainly on the population of 4d state therefore **Figure 4** represents the time evolution of the population of this state in the presence and absence of Tri atomic ions formation is shown by curves (a, b and c) and (a^- , b^- and c^-) respectively. The saturation behavior shown up to 250 ns reflects the less contribution of the Tri atomic ions formation during this period. Moreover the increase of the 4d population density at the higher atomic density (2 × 1012 cm^{-3}) over the time interval 400 - 500 ns gives an evidence for the formation of Tri atomic ions. On the other hand the omission of this process leads to the decrease of 4d population density as shown by curves (a^-, b^- and c^-). As this process produced in laser ionization based on resonance saturation and this technique depends mainly on the saturation of 3p state of Sodium atoms therefore one expect associative ionization to take place among the atoms of this saturated level.

3.3. The Time Evolution of Electron Energy Distribution Function

For a deeper understanding of the effect of formation Na_3^+ on time evolution of plasma formation calculations are performed first to obtained the EEDF in the presence and absence of this process at different time intervals at atomic density (2×10^{12} cm^{-3}). This is shown in **Figure 5**. In this figure the number of peaks appeared over the whole electron energy range can be illustrated as follows. The peak A represent electrons at energy about 0.27 eV generated by associative ionization (AI), the peaks B and C represent electrons of energy about 0.87 eV generated by penning ionization. While peaks D and E refers to electrons which are generated by associative and penning ionization and heated up by the first and second super elastic collision processes respectively. The peak F corresponds to electrons resulted by penning ionization and heated up through first and second super elastic collision process [2] [8].Comparison between (i) and (ii) in **Figure 5** shows that: the inclusions of tri-atomic associative ionization reaction leads only to the increase of the values electron energy distribution Function.

This appears from the values of the peaks. This means that this reaction is not affecting the processes which are taking place in its absence. This result can be drawn from the constant location of the peaks in the two parts of the **Figure 5**. To give a deeper understanding about the time at which this reaction occurs. **Figure 6** show that

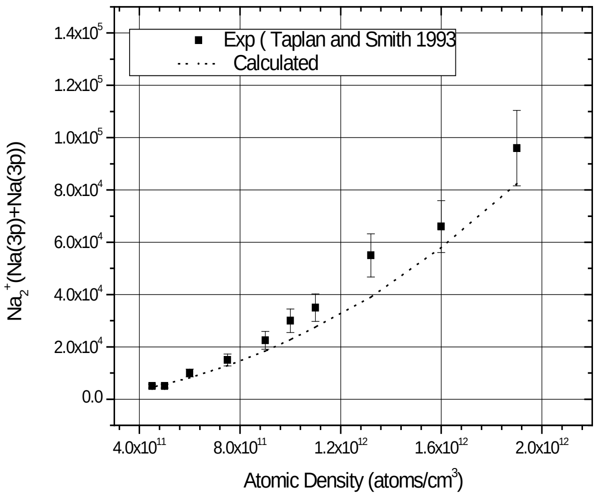

Figure 2. Na_2^+ ion yield versus atomic density.

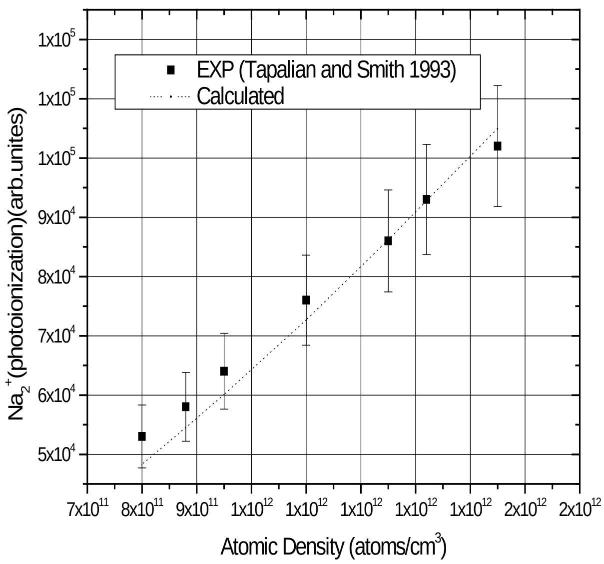

Figure 3. Na_2^+ ion yield (photoionization of Na_2) atomic density.

the omission of this reaction does not affect.

Also the position of the peaks on the energy axis but rather it increases the electron density over the energy range from 0.87 eV to 1.7 eV. This in turn results in a broadening of peaks B and C *i.e.* it increases the electrons density which is generated through Penning ionization process. Meanwhile it is noticed here that this reaction takes place during the early time interval 100 ns and becomes more effective as the time increases.

4. Conclusions

A modified previously developed a model of dense sodium vapor ionization induced by nanosecond resonant laser pulses exciting the 3S→3P is applied to study the effect of Na_3^+ formation on the generated plasma. Kinetics of the processes which produce the molecular ion Na_2^+ and the tri-atomic ion Na_3^+ in lasers excited sodium vapor was investigated theoretically. Formation of Na_3^+ results in an increase of the electron energy distribution function and hence the electron density which generates more density plasma in other words leads to full ionization of the atomic vapor. The results showed non-Maxwell Ian distribution of the electrons for differ-

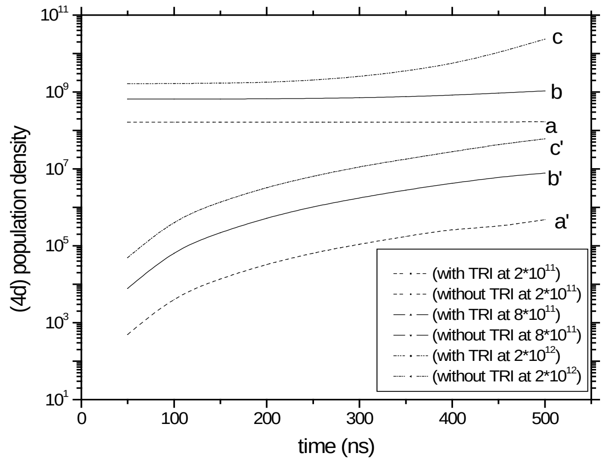

Figure 4. The time evolution of population density of 4d level.

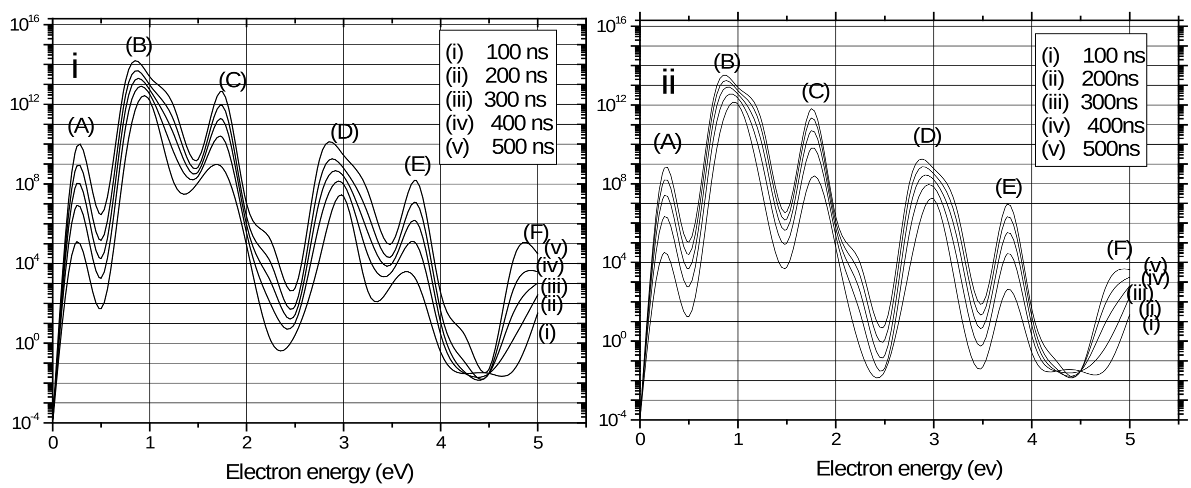

Figure 5. Electron energy distribution function calculated at different time intervals for sodium atomic density of 2×10^{12} in (i) Presence of tri atomic associative ionization process; (ii) Absence tri-atomic associative ionization process.

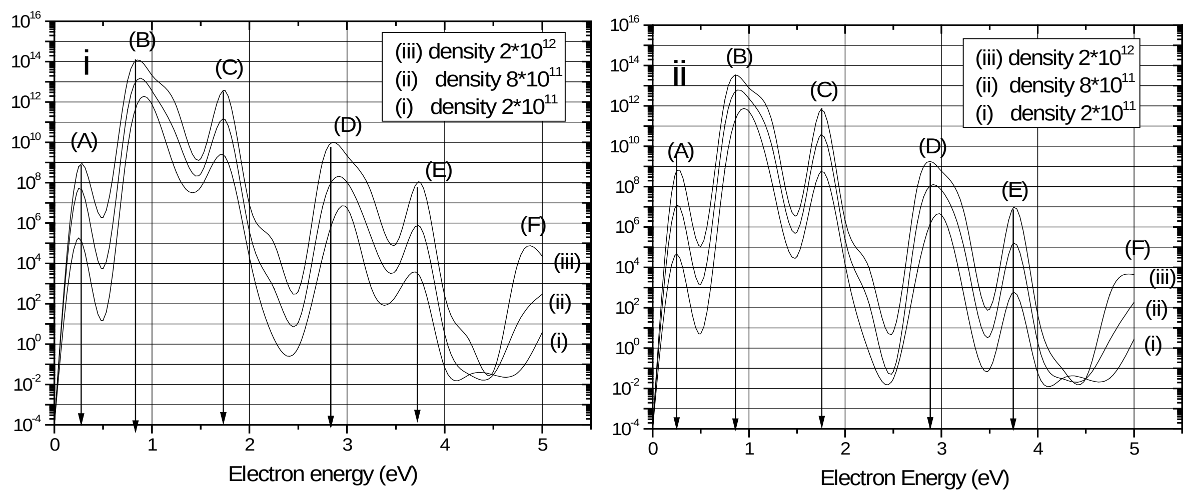

Figure 6. Electron energy distribution function calculated for different values of sodium atomic density in (i) Presence of tri-atomic associative ionization process; (ii) Absence of tri-atomic associative ionization process.

ent values of sodium vapor densities. The collisional ionization processes such as the associative ionization and Hornbeck-Molnar ionization play the important rule in producing the molecular ion density Na_2^+. The good agreement shown in compare the calculated and measurement values of the formed Na^{3+} and Na^{2+} reveled the validity of the model in investigated the plasma generation using LIBORS technique.

References

[1] Lucatorto, T.B. and McIlrath, T.B. (1976) Efficient Laser Production of a Na^+ Ground-State Plasma Column: Absorption Spectroscopy and Photoionization Measurement of Na^+. *Physical Review Letters*, **37**, 428. http://dx.doi.org/10.1103/PhysRevLett.37.428

[2] Carre, B., Roussel, F., Spiess, G., Bizau, J.M., Gerard, P. and Wuilleumier, F. (1986) *Zeitschrift für Physik D Atoms, Molecules and Clusters*, **1**, 79.

[3] Stacewicz, T., Gorbunov, N.A. and Kozlowski, P. (1998) Excitation of Sodium Atoms by 330-nm Laser Pulses. *Applied Physics B*, **66**, 461-465. http://dx.doi.org/10.1007/s003400050419

[4] Leonov, A.G., Chekhov, D.I. and Starostin, A.N. (1997) Mechanisms of Resonant Laser Ionization. *JETP*, **84**, 703-715. http://dx.doi.org/10.1134/1.558204

[5] Gorbunov, N.A., Grochola, A., Kruk, P., Pietruczuk, A. and Stacewicz, T. (2002) Studies of Electron Energy Distribution in Plasma Produced by a Resonant Laser Pulse. *Plasma Sources Science and Technology*, **11**, 492. http://dx.doi.org/10.1088/0963-0252/11/4/316

[6] Kosarev, N.I. and Shaparev, N.Ya. (2006) Resonance Laser-Induced Ionisation of Sodium Vapour Taking Radiative Transfer into Account. *Quantum Electronics*, **36**, 369. http://dx.doi.org/10.1070/QE2006v036n04ABEH013153

[7] Tapalian, C. and Smith, W.W. (1993) *Chemical Physics Letters*, **211**, 425.

[8] Mahmoud, M.A. (2005) Electron Energy Distribution Function in Laser-Excited Rubidium Atoms. *Journal of Physics B*: *Atomic*, *Molecular and Optical*, **38**, 1545. http://dx.doi.org/10.1088/0953-4075/38/10/012

[9] Mahmoud, M.A. and Gamal, Y.E.E. (2012) Kinetics of Plasma Formation in Sodium Vapor Excited by Nanosecond Resonant Laser Pulses. *Indian Journal of Physics*, **86**, 659-666. http://dx.doi.org/10.1007/s12648-012-0093-3

[10] Measures, R.M. (1977) Efficient Laser Ionization of Sodium Vapor—A Possible Explanation Based on Superelastic Collisions and Reduced Ionization Potential. *Journal of Applied Physics*, **48**, 2673. http://dx.doi.org/10.1063/1.324135

[11] Vriens and Smeets, A.H. (1980) *Physical Review A*, **22**, 940.

[12] Drawin, H.N. and Felenbok, P. (1965) Data for Plasma in Local Thermodynamic Equilibrium. Gauthier-Villarrs, Paris.

[13] Kushawaha, S.V. and Leventhal, J.J. (1982) Associative Ionization in Laser-Excited Sodium Vapor. *Physical Review A*, **25**, 346. http://dx.doi.org/10.1103/PhysRevA.25.346

[14] Babenko, E., Tapalian, C. and Smith, W.W. (1995) Associative Ionization in Laser-Excited Sodium 3p+3d Collisions. *Chemical Physics Letters*, **244**, 121-126. http://dx.doi.org/10.1016/0009-2614(95)00878-8

[15] Allegrini, M., Alzetta, G., Kopystynska, A., Moi, L. and Orriols, G. (1976) Electronic Energy Transfer Induced by Collision between Two Excited Sodium Atoms. *Optics Communications*, **19**, 96-99. http://dx.doi.org/10.1016/0030-4018(76)90394-1

[16] Huennekens, J. and Gallagher, A. (1983) Cross Sections for Energy Transfer in Collisions between Two Excited Sodium Atoms. *Physical Review A*, **27**, 771. http://dx.doi.org/10.1103/PhysRevA.27.771

[17] Aymar, M., Luc-Koenig, E. and Combert-Farnoux, F. (1976) Theoretical Investigation on Photoionization from Rydberg States of Lithium, Sodium and Potassium. *Journal of Physics B*: *Atomic and Molecular Physics*, **9**, 1279. http://dx.doi.org/10.1088/0022-3700/9/8/013

[18] Laughlin, C. (1978) One- and Two-Photon Ionisation of the 3s and 3p States of Na I. *Journal of Physics B*: *Atomic and Molecular Physics*, **11**, 1399. http://dx.doi.org/10.1088/0022-3700/11/8/011

[19] Geltman, S. (1977) *Journal of Physics B*: *Atomic and Molecular Physics*, **10**, 3507.

[20] Bezuglov, N.N., Klyucharev, A.N. and Sheverev, V.A. (1987) Associative Ionisation Rate Constants Measured in Cell and Beam Experiments. *Journal of Physics B*: *Atomic and Molecular Physics*, **20**, 2497. http://dx.doi.org/10.1088/0022-3700/20/11/018